Editors' Suggestion

Viscous free-surface cusps: Local solution

J. Eggers
School of Mathematics, University of Bristol, Fry Building, Woodland Road, Bristol BS8 1UG, United Kingdom

(Received 20 June 2023; accepted 6 November 2023; published 6 December 2023)

Free-surface cusps appear as a generic feature in viscous flow with a free surface. However, a mathematical description has so far only been possible by constructing exact solutions to the Stokes equation in very specific and idealized geometries, using complex mapping techniques. Here we use the boundary integral formulation of the Stokes equation to show that cusps are local singular solutions to Stokes' equation. We recover Jeong and Moffatt's [J. Fluid Mech. **241**, 1 (1992)] local cusp solution in the limit of diverging cusp curvature, demonstrating its universality across all viscous flows.

DOI: 10.1103/PhysRevFluids.8.124001

I. INTRODUCTION

Free-surface cusps appear widely in viscous flow problems [1] whenever the flow is strongly forced in an approximately two-dimensional manner, and such that viscous forces are comparable to surface tension forces. This balance is quantified by the dimensionless capillary number $\mathrm{Ca} = U\eta/\gamma$ being of order unity or larger, where U is a typical flow speed, η the fluid viscosity, and γ the coefficient of surface tension. On the right of Fig. 1 we show a cusp with a rounded tip, as found from a local analysis of Jeong and Moffatt's exact solution [2], and whose curvature increases exponentially with capillary number. The goal of this paper is to derive this structure directly from a local analysis of Stokes' equation.

Cusps have been demonstrated experimentally in a variety of geometries, for example by dragging fluid with two rollers [2,3] or a single roller [4], or by pouring a jet of viscous liquid into a bath of the same liquid [5–7]. Theoretically, exact solutions of the two-dimensional Stokes equation showing cusping have been found by placing singularities underneath a free surface [2,8–10], or next to a two-dimensional "drop" [11,12]. More exact solutions displaying cusping behavior were found placing a dipole next to a bubble [13], or adding suction [14].

Free-surface cusps deserve particular interest since they can serve as channels through which air can enter into a fluid, as shown theoretically [5,6] and experimentally [4,6]. Thus, cusps are of broad interest for air entrainment in jets and waves [15], as well as coating flows [16].

It is important to distinguish cusps, which are quasi-two-dimensional objects, and which become singular along a line, from conical tips, which form at the end of bubbles in a variety of flows [17–19], and which become singular at a point. Available experimental evidence indicates that cusps occur when the driving flow becomes sufficiently two-dimensional, for example, when a rising bubble is close to a wall. It is also known that a sufficiently large bubble rising in a *viscoelastic* liquid breaks axisymmetry to form a "knife-edge" ending in a cusp at its rear [20].

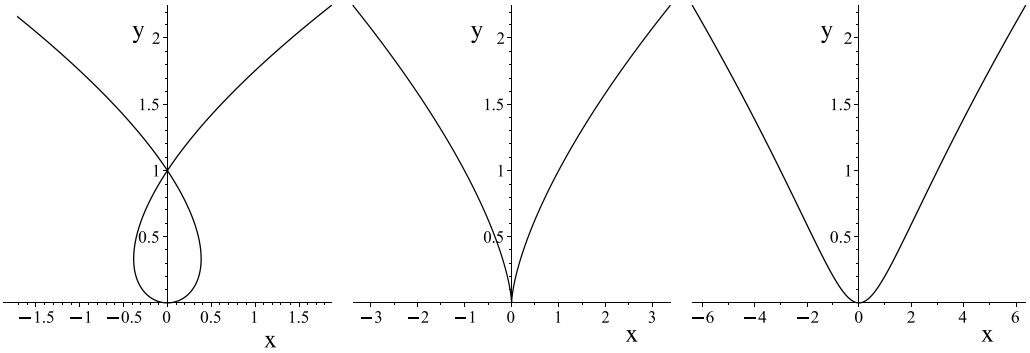

FIG. 1. A cusp can be understood as arising when a loop in a smooth curve is formed. We plot $x = \delta\varphi + c\varphi^3/3$, $y = \varphi^2/2$, for $c = 1$. On the left, $\delta < 0$, and the curve self-intersects, so the mapping is no longer invertible. In the middle, the critical state of $\delta = 0$ is shown, for which the curve is a cusp $x \propto y^{3/2}$. On the right, $\delta > 0$, and the curve has opened to produce a cusp in the far field, but being rounded at the tip. Physically, a cusp at finite capillary number corresponds to a rounded tip, whose curvature increases exponentially with the capillary number [2]. Thus, formally the singular cusp in the middle occurs in the limit of infinite capillary number.

Most of the theoretical information we have about the structure of cusps comes from an analysis of exact solutions, found by mapping the fluid domain onto the unit disk. A cusp singularity of the free surface occurs when the map becomes noninvertible on the unit circle, corresponding to the free surface. This means the viscous cusp singularity has a very simple, highly universal structure, associated with an exponent of $3/2$, when the width of the cusp is plotted as a function of the distance from the tip [21,22].

Other physical examples, which share the self-similar structure with viscous cusps, appear in elasticity (the Hertz solution [23] and elastic folds [24]), biology [25], optics [26], relativistic membranes [27], shock formation [28], and contact line motion [29]. These "geometrical" singularities [22] are to be distinguished from other cusp solutions, such as the cusp that arises from the touching of two smooth surfaces (the viscous coalescence problem [34]), for which the cusp width scales like the distance from the tip to the power 2. The same far-field exponent 2 is observed for cusps formed by steep capillary waves [22].

However, although the surface shape often follows from simple geometrical considerations and is thus common to many different problems, the underlying physics, and in particular the underlying bulk motion away from the interface, is nontrivial, and can be quite different from problem to problem. It therefore remains to be shown for each individual case that the cusp structure follows from the equations of motion. It is this we will undertake in this paper for the case of Stokes' equation with a free surface.

A first step in this direction was taken in Ref. [3], where the $3/2$ power-law form of the cusp was calculated by a local expansion of Stokes' equation. However, this leaves open the structure of the tip, which is an important issue, since a truly singular tip would lead to a force singularity, which would produce a logarithmically infinite energy dissipation [3]. This issue was resolved by Jeong and Moffatt in Ref. [2], who showed that in their exact solution the tip was rounded on a scale exponentially small in the capillary number, making the energy dissipation finite.

An alternative approach to the cusp problem was taken in Refs. [30–32], where the slenderness of the cusp shape was exploited to formulate an effective "codimension-two" boundary value problem, similar to the classical lubrication approach of Reynolds [33]. This boundary value problem has to be matched to an inner problem describing the tip of the cusp, to avoid the problems encountered by Ref. [3]. A great advantage of this approach is that it applies to a much more general class of cusp problems, for example the coalescence of viscous cylinders, also treated initially by constructing

exact solutions using mapping techniques [34,35]. In addition, the same idea has been applied to problems involving Laplace's equation, such as water entry, and Hele-Shaw flow [30]. However, the stationary cusp of Jeong and Moffatt [2] has not been addressed explicitly.

As the starting point of our calculation we now derive the asymptotic form of the free-surface shape of a cusp based on the idea that the parametric form of the curve $(x(\varphi), y(\varphi))$ is no longer invertible. This is motivated by Jeong and Moffatt's analysis, who for a free-surface flow forced by a vortex dipole, find a smooth mapping $z = w(\zeta)$ of the unit disk onto the flow domain. A cusp singularity occurs when a point with $w'(\zeta) = 0$ approaches the unit circle from the outside. In terms of the parametric representation, such a singularity corresponds to $x'(\varphi) = y'(\varphi) = 0$ [22] somewhere on the curve. The simplest, generic form of this singularity occurring at $\varphi = 0$ is (after appropriate rotations and rescaling) $x = c\varphi^3/3$ and $y = \varphi^2/2$, which reproduces the expected 3/2 scaling; the cusp has been oriented in the positive y-direction. The constant c provides a scale for the width of the cusp, and is a nonuniversal quantity depending on each individual flow configuration, as we will see below.

The generic perturbation to this singular shape (all other perturbations can again be eliminated by trivial transformations [1]) is $x = \delta\varphi + c\varphi^3/3$, $y = \varphi^2/2$, as shown in Fig. 1. For $\delta > 0$ this yields a rounded tip, as shown on the right of Fig. 1, for $\delta < 0$ the figure self-intersects, while for $\delta = 0$ the singular cusp is seen.

For the purposes of our calculation, we expand in the size $\kappa^{-1} \equiv \epsilon^2$ of the cusp tip, where κ is the curvature at the tip, written in suitable units of length. In the example presented by Jeong and Moffatt, this would be the distance of the singularity driving the flow from the free surface. With these conventions, the cusp solution becomes

$$x = \epsilon^2\big(\psi + \epsilon c\psi^3/3\big), \quad y = \epsilon^2\psi^2/2, \tag{1}$$

which has a curvature $d^2y/dx^2 = y''/x'^2 = \epsilon^{-2} = \kappa$ at the tip, as required. In the scaling of Eq. (1), taking the limit $\epsilon \to 0$ at constant ψ yields the tip region of the cusp, described by $x = \epsilon^2 y/2$. However, putting $\psi = \sigma/\sqrt{\epsilon}$, we obtain

$$x = \epsilon^{3/2}\big(\sigma + c\sigma^3/3\big), \quad y = \epsilon\sigma^2/2, \tag{2}$$

which has the form of a similarity solution. Exactly the same form of solution is obtained from the exact solution [2], for a particular value of c. We conclude that there are three relevant scales in our problem, as sketched in Fig. 2. In Eq. (1), ψ values $O(1)$ describe the tip, whereas σ values $O(1)$ describe the cusp. Finally, there is a nonuniversal outer length scale.

The purpose of this paper is to show that the full self-similar solution (1) or (2), written in units of the curvature and with c a free parameter, satisfies Stokes' equation. This is done using the boundary integral method, which involves integrals over the interface. To this end we still need to find the tangential velocity along the interface, which we do by calculating the limiting behavior of the exact solution found by Jeong and Moffatt on the inner and intermediate scales.

We will see that in the limit $\epsilon \to 0$ the integral equation splits into closed sets of equations on two different scales: the tip (inner) and the cusp (intermediate) scale. At the tip scale, shown in the inset of Fig. 2, the integral equation closes. This means the dominant contribution to the integrals comes from the leading order, parabolic part of Eq. (1), the remainder is subdominant. At the cusp scale, shown as the dashed line in Fig. 2, the main driving comes from the highly curved tip region (inset). However, there are also local contributions within the cusp region itself, which account for the presence of an interface.

In Sec. II, we set up the integral equation and find the velocity. In Secs. III and IV, we calculate the limits of the boundary integral equation appropriate for the tip and cusp regions, respectively. For both regions, we then show that Eq. (1) is a solution.

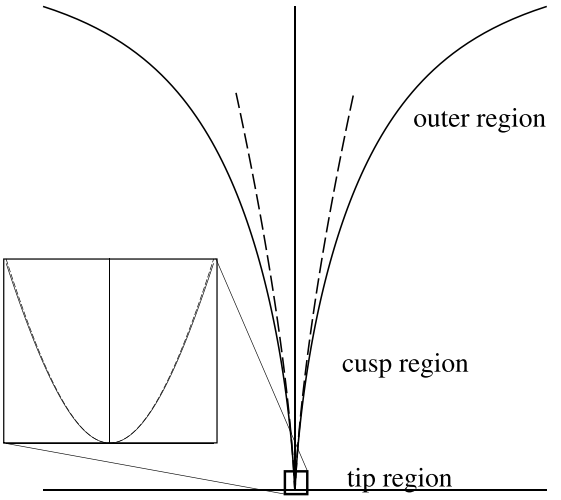

FIG. 2. A sketch of the scaling regions relevant for our calculations; the solid line is the exact solution of Jeong and Moffatt [2], the dashed line is Eq. (1), with $c = 3^{3/2}/4$ to fit the Jeong-Moffatt solution (cf. Appendix A). The inner tip region is the scale on which the tip is rounded and is found keeping $\psi = O(1)$ as $\epsilon \to 0$ in Eq. (1). The integral equation is closed on the scale of the tip, as shown in Sec. III. The intermediate cusp region is described by Eq. (2) and is recovered keeping σ constant. Here the dominant contribution to the J integral (see Sec. II) is nonlocal and comes again from the tip region. Finally, the outer solution depends on the particular problem at hand, and is found for $\psi = \phi/\epsilon$, where ϕ is held fixed.

II. THE INTEGRAL EQUATION

Boundary integral equations [36,37] can be used to describe Stokes (viscously dominated) flow for an arbitrary combination of solid and free surfaces. The advantage is that they require information about the bounding surfaces only, in the case of a free surface (such as a bubble in an external flow) the value of the velocity field on the surface. While boundary integral equations have been used primarily for numerical purposes, here, following Refs. [19,38], they are the starting point for an analytical treatment. The key idea is to make use of insight into the structure of the free surface, to write the boundary integral as an ordinary one-dimensional integral.

Since we are interested in a small neighborhood around a free-surface cusp only, here we restrict ourselves to the integral equation for a single free surface, which in units of $v_\eta = \gamma/\eta$ reads [39]

$$\frac{\mathbf{v}(\psi_1)}{2} = -\int_{-\infty}^{\infty} \kappa \mathbf{J}\cdot\hat{\mathbf{n}}\mathrm{d}\psi_2 - \int_{-\infty}^{\infty} \mathbf{v}\cdot\mathbf{K}\cdot\hat{\mathbf{n}}\mathrm{d}\psi_2 + \mathbf{v}^{(\mathrm{ext})}(\psi_1), \tag{3}$$

where ψ is used to parametrize the interface as $\mathbf{x}(\psi)$, and $\mathbf{v}(\psi)$ is a shorthand for $\mathbf{v}[\mathbf{x}(\psi)]$. For convenience, we have written the boundary integral as an integral over the real line, and we assume that the surface can be closed at infinity to produce a closed surface, as required by the boundary integral method. The vector $\hat{\mathbf{n}} = (y_\psi, -x_\psi)$ points in the direction of the outward normal; with this choice, the parameter ψ used as integration variable is arbitrary.

In Eq. (3), defining $\mathbf{r} = \mathbf{x}_1 - \mathbf{x}_2$ and $r = |\mathbf{r}|$, kernels are defined by

$$\mathbf{J}(\mathbf{r}) = \frac{1}{4\pi}\left[-\mathbf{I}\ln r + \frac{\mathbf{rr}}{r^2}\right], \qquad \mathbf{K}(\mathbf{r}) = -\frac{1}{\pi}\frac{\mathbf{rrr}}{r^4}, \tag{4}$$

which are the Green's functions of the two-dimensional Stokes equation. This means that $\mathbf{J}\cdot\mathbf{F}$ is the velocity generated at $\mathbf{x}_1$ by a point force $\mathbf{f} = \mathbf{F}\delta(\mathbf{x}_1 - \mathbf{x}_2)$, located at $\mathbf{x}_2$ (the "Stokeslet"), while

$\mathbf{K}\cdot\mathbf{F}$ is the stress (the "stresslet"), and

$$\kappa = \frac{x_\psi y_{\psi\psi} - y_\psi x_{\psi\psi}}{\left(x_\psi^2 + y_\psi^2\right)^{3/2}}$$

is the curvature. The contribution $\mathbf{v}^{(\mathrm{ext})}$ is an externally applied velocity, which depends on the problem, and which does not affect the local structure of the solution. In the solution of Ref. [2] it is a vortex dipole, placed underneath the free surface. More generally, one can think of $\mathbf{v}^{(\mathrm{ext})}$ as the flow generated by all the stresses not represented by the first integral in Eq. (3), expanded to leading (monopole) order around the position of the cusp.

We are looking for *stationary* solutions, which implies that the interface is a streamline. Consequently, the velocity along the interface can be written

$$\mathbf{v} = u_0\mathbf{t}, \quad \mathbf{t} = \frac{(x_\psi, y_\psi)}{\sqrt{x_\psi^2 + y_\psi^2}}, \tag{5}$$

with $\mathbf{t}$ the (normalized) tangent vector. The mathematical problem to be solved in this paper consists in solving the simultaneous equations (3) and (5) for an interface shape $\mathbf{x}(\psi)$, as well as for the tangential velocity $u_0(\psi)$.

We aim to solve Eq. (3) in the limit $\epsilon \to 0$. The most obvious strategy would be to rewrite Eq. (3) in terms of the similarity variable σ of Eq. (2). However, expanding κ at constant σ yields

$$\kappa = \epsilon^{-1/2}\frac{1 - c\sigma^2}{\sigma^3} + O(\epsilon^{3/2}),$$

which is singular at the tip as $\sigma \to 0$. Instead, we must resolve the interface on scale ψ, for which

$$\kappa_0 = \frac{\epsilon^{-2}}{(1+\psi^2)^{3/2}} \tag{6}$$

as $\epsilon \to 0$, which is now regular for arbitrary ψ, up to an overall scale factor ϵ^{-2}.

Thus, we solve Eq. (3) in two steps: first we solve for the flow near the tip, by taking the limit $\epsilon \to 0$ at constant ψ_1. Since the integral extends over all scales, we must consider ψ_2 varying over all scales. However, our analysis reveals that to leading order, all contributions (apart from constants), come from a region of $O(1)$ in ψ_2. In particular, the constant c does not come into play at this order, since its contribution in Eq. (1) is of higher order in ϵ. To find the tangential velocity u_0 on this scale, we can analyze the Jeong-Moffatt solution, as explained in more detail in Appendix A 2. Starting from Eq. (A4), putting $\theta = \pi/2 - \sqrt{3}\epsilon\psi$, and taking the limit $\epsilon \to 0$, using the approximation (A5), one finds

$$u_0(\psi) = -\frac{1}{\pi}\mathrm{arcsinh}(\psi) = -\frac{1}{\pi}\ln\left(\sqrt{1+\psi^2} + \psi\right) \tag{7}$$

to leading order in ϵ. In Sec. III below we confirm that Eq. (7), together with $x = \epsilon^2\psi$, $y = \epsilon^2\psi^2/2$, is a solution of the integral equation (3), to leading order $O(1)$ in ϵ.

To characterize the cusp, in Sec. IV we put $\psi = \sigma/\sqrt{\epsilon}$ and take the limit $\epsilon \to 0$ at constant σ. Analyzing the integral over ψ_2, in addition to the tip region the contributions now come from $\psi_2 = \sigma_2/\sqrt{\epsilon}$, where $\sigma_2 = O(1)$. To leading order, the tangential velocity (7) is now

$$u_0 = \frac{1}{2\pi}\ln\left(\frac{\epsilon}{4\sigma^2}\right), \tag{8}$$

and the interface is given by (2), with arbitrary c. The dependence of u_0 on σ, $u_0 \sim -\ln(\sigma)/\pi$, corresponds to the flow generated by an upward force of strength 2γ, located at the tip of the cusp, as suggested by J. Hinch, see the Appendix to [2].

III. THE TIP REGION

To investigate the tip, we hold ψ_1 constant and let $\epsilon \to 0$; the interface is described by (1). We obtain for the left-hand side of Eq. (3):

$$\frac{\mathbf{v}}{2} = u_0(\psi_1)\frac{(1, \psi_1)}{2\sqrt{1+\psi_1^2}}, \tag{9}$$

so for both components, the leading order is $O(\epsilon^0)$. Expanding the integrand $f \equiv \kappa \mathbf{J} \cdot \hat{\mathbf{n}}|_{x/y}$ into a power series in ϵ [and similarly for the K integral in Eq. (3)], we obtain an *inner* expansion

$$f \approx \sum_{n=0}^{Q} f_n(\psi_2)\epsilon^n \equiv I_Q f, \tag{10}$$

using the notation of, e.g., Eq. [40].

However, the integrals over $f_1(\psi_2)$ (as well as higher-order coefficients) are divergent for $\psi_2 \to \infty$, indicating a nonuniform behavior of the integrand as $\epsilon \to 0$. Thus, we have to combine Eq. (10) with an *outer* expansion [41],

$$f \approx \sum_{n=1}^{Q+1} F_n^{\pm}(\phi_2)\epsilon^n \equiv O_{Q+1} f, \tag{11}$$

where now $\psi_2 = \phi_2/\epsilon$, with ϕ_2 held constant. In the outer expansion, we have to go to higher order than in Eq. (10), to guarantee a contribution of the same order to the integral, considering that the integration variable is now ϕ instead of ψ. The two signs $\pm$ correspond to expansions for $\phi_2 > 0$ and $\phi_2 < 0$, respectively. Since ψ_1 only appears in the combination $\psi_2 - \psi_1 = \phi_2/\epsilon - \psi_1$, the leading order contribution $F_1^{\pm}(\phi_2)$ is independent of ψ_1.

From the two expansions (10) and (11) one can construct a composite solution $f \approx I_Q f + O_{Q+1} f - I_Q O_{Q+1} f$, using that $I_Q O_{Q+1} f = O_{Q+1} I_Q f$ [42]. Since we only want to solve (3) to leading order $O(\epsilon^0)$, we only have to consider the case $Q = 0$; it turns out that the overlap integral $O_1 I_0 f$ vanishes for both components of the J and K integrals, so we compute

$$\int_{-\infty}^{\infty} f(\psi_2, \epsilon) d\psi_2 \approx \int_{-\infty}^{\infty} f_0(\psi_2) d\psi_2 + \int_{-\infty}^{0} F_1^{-}(\phi_2) d\phi_2 + \int_{0}^{\infty} F_1^{+}(\phi_2) d\phi_2, \tag{12}$$

remembering that $d\phi_2 = \epsilon d\psi_2$, so both inner and outer expansions contribute at leading order. However, the outer expansion only contributes a ψ_1-independent constant (which vanishes for the x component), but which only sets the curvature $\kappa = \epsilon^{-2}$ as we will see. Also note that the outer solution (scale ϕ_2) is no longer universal, but depends on the individual problem. In other words, on the tip scale we have

$$\frac{u_0(\psi_1)}{2\sqrt{1+\psi_1^2}} = -J_x^{(in)}(\psi_1) - K_x^{(in)}(\psi_1) \tag{13}$$

$$\frac{u_0(\psi_1)\psi_1}{2\sqrt{1+\psi_1^2}} = -J_y^{(in)}(\psi_1) - K_y^{(in)}(\psi_1) + J_y^{(in)}(0) + K_y^{(in)}(0), \tag{14}$$

where in Eq. (14) we have subtracted the integrals for $\psi_1 = 0$, so the aforementioned constants drop out, and both sides vanish for $\psi_1 = 0$. The superscript (in) refers to the integral over the inner expansion, the first integral on the right-hand side of Eq. (12).

The important insight of our asymptotic analysis so far is that in the limit $\epsilon \to 0$, the boundary integral equation (3) reduces to a closed equation for the tip of the cusp, of size $\kappa^{-1} = \epsilon^2$. The inner expansion (13), (14) does not contain any parameters, and is thus guaranteed to be satisfied by virtue of the global exact solution [2]. In Appendix B 1, we have confirmed this result by evaluating

the integrals appearing in Eq. (13) for any ψ_1. This establishes that a tip of the form $y = x^2/(2\epsilon^2)$, together with the tangential velocity (7), is a universal feature of any sharp tip in viscous two-dimensional Stokes flow, regardless of the geometry or external driving.

Addressing the constants appearing in Eq. (14), which have been subtracted, we evaluate the y component of Eq. (3) at $\psi_1 = 0$, which for $\epsilon \to 0$ has the form

$$v^{(ext)}(0) = J_y^{(in)}(0) + K_y^{(in)}(0) + J_y^{(out)}(0) + K_y^{(out)}(0), \tag{15}$$

where the superscript (out) refers to the integral over the outer expansion, the second and third integrals on the right-hand side of Eq. (12). The right-hand side of Eq. (15) has the form $a + b \ln \epsilon$, whose origin lies in the integrand of $J_y^{(\mathrm{in})}(0)$. Its dominant contribution is [cf. Eqs. (3) and (6)]

$$\frac{\kappa_0}{4\pi} x_\psi \ln r = \frac{\epsilon^{-2}}{4\pi(1+\psi^2)^{3/2}} \epsilon^2 2 \ln \sqrt{\epsilon},$$

so that its integral over ψ_2 becomes $J_y^{(\mathrm{in})}(0) = \ln \epsilon/\pi$ [cf. Appendix B 2, Eq. (B9)]. This means that the velocity has a contribution proportional to $\ln \epsilon$, and thus the K-integrals, which contain u_0, in general will have such a contribution as well.

In Appendix B 2 we show, using Jeong and Moffatt's exact solution, that Eq. (15) is indeed satisfied exactly (in particular, the left-hand side of Eq. (15) is also of the form $a_1 + b_1 \ln \epsilon$). While the contributions from the inner expansions, $J_y^{(\mathrm{in})}(0)$ and $K_y^{(\mathrm{in})}(0)$, are universal numbers, the contributions $J_y^{(\mathrm{out})}(0)$ and $K_y^{(\mathrm{out})}(0)$ come from an integral over the entire surface. They are therefore not universal, and will be different, depending on the problem at hand.

Another way to look at the same statement is to define the capillary number in terms of the external flow, i.e. the y-component of the external velocity, which would be generated in the absence of an interface. In that case $\mathrm{Ca} = v^{(\mathrm{ext})}(0)$ (in units of the capillary speed), evaluated at the position of the cusp. If now the integrals on the right-hand side of Eq. (15) are of the form $a + b \ln \epsilon$, and remembering that $\epsilon = \sqrt{\kappa}$ in units of the distance between free surface and the dipole, then one obtains

$$\kappa = e^{-2a/b} e^{2\mathrm{Ca}/b}. \tag{16}$$

Thus, one finds exponential growth of the curvature with flow strength [2], but the coefficients are not universal. In the particular case treated in Ref. [2], one finds [cf. Eq. (B8)]

$$a = \frac{9}{16\pi} \ln \frac{\sqrt{3}}{16}, \quad b = \frac{9}{16\pi},$$

so that

$$\kappa_{JM} = \frac{3}{256} e^{32\pi \mathrm{Ca}/9}. \tag{17}$$

If the capillary number is measured instead in terms of the strength α of the vortex dipole driving the flow, namely $\mathrm{Ca}_d = \eta\alpha/(\gamma d^2)$, then we have $\mathrm{Ca} = 9\mathrm{Ca}_d$, and Eq. (17) agrees with the result of Ref. [2]; here d is the distance of the dipole from the unperturbed interface.

A more universally applicable way to define the capillary number is to include the effect of the interface. Following Ref. [2], we consider the limit $\lim_{|x|\to 0} \lim_{\epsilon \to 0} \frac{u_0}{\ln \epsilon}$, which (in units of $v_\eta \ln \epsilon$) measures the speed of the fluid sweeping past the cusp. In our language, this corresponds to taking the limits $\epsilon \to 0$ at constant ϕ, then $\phi \to 0$. As can be seen from Eq. (7), putting $\psi = \phi/\epsilon$, in the limit $\epsilon \to 0$ we obtain

$$\lim_{\phi \to +0} \lim_{\epsilon \to 0} \frac{u_0}{\ln \epsilon} = \frac{1}{\pi}. \tag{18}$$

Indeed, Eq. (18) is confirmed by considering the uniformly valid approximation (A8) of the tangential velocity, with a correction $O(\phi^2)$ in the limit $\phi \to 0$. Keeping in mind that $\alpha \approx -\ln \epsilon/(16\pi)$,

this is consistent with the limit of ± 16, found by Ref. [2]. In accordance with Eq. (7), the capillary number based on the actual flow speed along the cusp face is $\mathrm{Ca}_{\mathrm{cusp}} = -\ln\epsilon/\pi + C$, where the constant C is arbitrary. Remembering that $\kappa \propto 1/\epsilon^2$ we find that

$$\kappa \approx \kappa_0 e^{2\pi \mathrm{Ca}_{\mathrm{cusp}}}, \tag{19}$$

where the prefactor κ_0 depends on the chosen units of length, and therefore cannot be universal.

IV. THE CUSP REGION

The above calculation on the scale of the tip only applies to the inner region for which $\psi = O(1)$, where in the limit $\epsilon \to 0$, $y = x^2\kappa/2$. Now we turn to the scale of the cusp, for which $\psi = \sigma/\sqrt{\epsilon}$ in Eq. (1), with σ fixed as ϵ goes to zero. We will see that evaluating J and K integrals requires different approximations, so we treat them separately.

A. *J* integrals

The J integrals can be evaluated in a similar fashion to that of the tip scale, but on account of the scaling $\psi = \sigma/\sqrt{\epsilon}$, we now expand in powers of $\sqrt{\epsilon}$. To represent the integrand to a required order, in addition to the previous inner and outer regions, we require a third intermediate region, so that the three different regions are defined on scales ψ_2 (inner), $\psi_2 = \sigma/\sqrt{\epsilon}$ (intermediate), and $\psi_2 = \phi/\epsilon$ (outer).

Thus, if f is the integrand, then we consider three different expansions to represent the integral to a given order:

$$f \approx \sum_{n=0}^{Q-1} f_n(\psi_2)\epsilon^{n/2} \equiv I_{Q-1}f, \quad f \approx \sum_{n=1}^{Q} \overline{f}_n(\sigma)\epsilon^{n/2} \equiv M_Q f, \quad f \approx \sum_{n=2}^{Q+1} F_n(\phi)\epsilon^{n/2} \equiv O_{Q+1}f.$$

The outer expansion is not universal, and therefore cannot be computed from the universal cusp solution. Note, however, that it only contributes a constant and therefore does not need to be considered, except for the calculation of κ.

We can now define inner and outer composite solutions by proceeding in two steps. First we construct two composite solutions using the inner and intermediate expansions, and the intermediate and outer expansions, respectively, which results in the intermediate composite solutions

$$I_{Q-1}f + M_Q f - I_{Q-1}M_Q f \equiv I_c f, \quad M_Q f + O_{Q+1}f - M_Q O_{Q+1}f \equiv O_c f. \tag{20}$$

The resulting two expansions are then combined to find a composite solution for the integral I valid everywhere:

$$I \approx I_c f + O_c f - M_Q I_c f, \tag{21}$$

where $M_Q I_c f = M_Q O_c f$, to any order of $\sqrt{\epsilon}$, set by Q.

Beginning with the left-hand side of Eq. (3),

$$\frac{\mathbf{v}}{2} = \frac{1}{4\pi}\ln\left(\frac{\epsilon}{4\sigma_1^2}\right)\left(\frac{1+c\sigma_1^2}{\sigma_1}\sqrt{\epsilon} + O(\epsilon^{3/2}), 1 + O(\epsilon)\right), \tag{22}$$

so we need the x component to $O(\sqrt{\epsilon})$ and the y component to $O(1)$. Analysis of the composite solution for the integrand of the J integral shows that the leading order $O(1)$ contribution cancels owing to symmetry; at the next order $O(\sqrt{\epsilon})$, only $I_{Q-1}f$ contributes to the composite solution with $Q = 2$. This yields [with corrections of $O(\epsilon)$]

$$\int_{-\infty}^{\infty} \kappa \mathbf{J}\cdot\hat{\mathbf{n}}|_x d\psi_2 = \int_{-\infty}^{\infty} I_1 f d\psi_2 = -\sqrt{\epsilon}\frac{1+c\sigma_1^2/3}{2\pi\sigma_1}\int_{-\infty}^{\infty}\frac{d\psi_2}{\left(1+\psi_2^2\right)^{3/2}} = -\sqrt{\epsilon}\frac{1+c\sigma_1^2/3}{\pi\sigma_1}, \tag{23}$$

the leading order contribution coming from the inner integral, corresponding to a point forcing by the tip curvature.

As for the y component of the J integral, the only contributions are from the inner and the outer expansions. This yields, putting $Q = 1$,

$$\int_{-\infty}^{\infty} \kappa \mathbf{J}\cdot\hat{\mathbf{n}}|_y d\psi_2 = \int_{-\infty}^{\infty} I_0 f d\psi_2 + \int_{-\infty}^{0} O_1^- f d\phi_2 + \int_0^{\infty} O_1^+ f d\phi_2 + O(\sqrt{\epsilon}).$$

Here the outer expansion only contributes a (σ_1-independent) constant, which is not universal. In fact, since the cusp scale is much smaller than the outer length scale, the outer contributions must be exactly the same as those found for the tip region. Thus, performing the inner integral, we find

$$\int_{-\infty}^{\infty} \kappa \mathbf{J}\cdot\hat{\mathbf{n}}|_y d\psi_2 = \frac{1}{4\pi}\left[\ln\left(\frac{\epsilon\sigma_1^2}{2}\right) - 1\right]\int_{-\infty}^{\infty} \frac{d\psi_2}{\left(1+\psi_2^2\right)^{3/2}} = \frac{1}{2\pi}\left[\ln\left(\frac{\epsilon\sigma_1^2}{2}\right) - 1\right] + J_y^{(\mathrm{out})}(0), \tag{24}$$

where $J_y^{(\mathrm{out})}(0)$ has been calculated in Appendix (B 2) for the case of the Jeong-Moffatt solution.

B. *K* integrals

To compute the x and y components of the K integral, another asymptotic region has to be considered, which comes from the factor r^4 in the denominator of the K integral [cf. Eq. (4)], becoming small as a function of ψ_2. Using Eq. (1) one finds $r^2 = (\psi_1 - \psi_2)^2\epsilon^4 D/9$, where

$$D = c^2(\psi_1^2 + \psi_1\psi_2 + \psi_2^2)^2\epsilon^2 + 6c(\psi_1^2 + \psi_1\psi_2 + \psi_2^2)\epsilon + 9\psi_1^2/4 + 9\psi_2\psi_1/2 + 9\psi_2^2/4 + 9.$$

The factor $(\psi_1 - \psi_2)^2$ in r^2 comes from the "local" contribution, where the integration variable equals the position along the interface where the velocity is computed. This does not lead to a singularity, since at the same point $\hat{\mathbf{n}}\cdot\mathbf{r} \sim (\psi_1 - \psi_2)^2$, $\mathbf{t}\cdot\mathbf{r} \sim \psi_1 - \psi_2$, and $r \sim \psi_1 - \psi_2$, so the zeros of numerator and denominator of the integrand cancel.

Instead, the main contribution to the K integral comes from a region of size $\Delta\psi_2 = O(1)$ around the minimum of D, instead of around the origin; the location of the minimum we denote by ψ_m. Putting $\psi_1 = \sigma_1/\sqrt{\epsilon}$, ψ_m is found from $dD/d\psi_2 = 0$. To leading order as $\epsilon \to 0$ this yields $9(\sigma_1/\sqrt{\epsilon} + \psi_2)/2 = 0$, so that $\psi_m = -\sigma_1/\sqrt{\epsilon} + O(\sqrt{\epsilon})$. To perform the integrals, we write the integrand IK of the K integral in the form $IK = N/D^2$. This means that putting $\Delta = \psi_2 - \psi_m$, we can expand the integrand in the form

$$IK = \frac{N}{D^2}, \quad D = D_0 + \frac{\Delta^2}{D_m} + O(\Delta^3). \tag{25}$$

From the definition of D, the functions D_0, D_m, and ψ_m can now be calculated in a power series in ϵ. Higher powers in Δ contribute a subleading contribution to the integral. Specifically, solving $dD/d\psi_2 = 0$ iteratively, we find

$$\psi_m = -\frac{\sigma_1}{\sqrt{\epsilon}} + \frac{4c\sigma_1}{9}s\sqrt{\epsilon} + O(\epsilon^{3/2}).$$

Neglecting contributions of order ϵ, we find (using the abbreviation $s = 3 + c\sigma_1^2$) $D_0 = s^2 + O(\epsilon)$, and $D_m = 4/9 + O(\epsilon)$.

Beginning with the x component of the K integral, the numerator can be expanded as $N(\psi_m + \Delta) = N_0(\Delta) + N_1(\Delta)\sqrt{\epsilon} + \ldots$, where N_0 is linear in Δ, and therefore gives a vanishing contribution. The next order in $\sqrt{\epsilon}$ is

$$N_1 = \frac{s^4}{2\pi^2\sigma_1}\ln\left(\frac{2\sigma_1}{\sqrt{\epsilon}}\right) + \frac{9s}{4\pi^2\sigma_1}\left[c\sigma_1^2\ln\left(\frac{2\sigma_1}{\sqrt{\epsilon}}\right) + s\right]\Delta^2,$$

so that using

$$\int_{-\infty}^{\infty}\frac{d\Delta}{D^2}=\frac{\pi}{3s^3},\quad \int_{-\infty}^{\infty}\frac{\Delta^2 d\Delta}{D^2}=\frac{4\pi}{27s},$$

we obtain

$$\int_{-\infty}^{\infty}\mathbf{v}\cdot\mathbf{K}\cdot\hat{\mathbf{n}}|_x d\psi_2\approx\sqrt{\epsilon}\int_{-\infty}^{\infty}\frac{N_1(\Delta)}{(D_0+\Delta^2/D_m)^2}d\Delta=\left[\frac{1+c\sigma_1^2/3}{\pi\sigma_1}+\frac{1+c\sigma_1^2}{2\pi\sigma_1}\ln\left(\frac{2\sigma_1}{\sqrt{\epsilon}}\right)\right]\sqrt{\epsilon}. \tag{26}$$

To check the size of the remainder, we expand

$$\mathbf{v}\cdot\mathbf{K}\cdot\hat{\mathbf{n}}|_x-\frac{N_1}{D^2}\sqrt{\epsilon}$$

in ϵ, using the outer scale $\psi_2=\phi_2/\epsilon$. The first nonvanishing contribution to this remainder is of order $\epsilon^{5/2}$, and thus subdominant.

In the same way, one can calculate the dominant contribution to the y component of the K integral, which is of the form (25) but with

$$N=N_0(\Delta)+O(\sqrt{\epsilon})=-\frac{27s}{8\pi^2}\ln\left(\frac{2\sigma_1}{\sqrt{\epsilon}}\right),$$

so now we have

$$\int_{-\infty}^{\infty}\mathbf{v}\cdot\mathbf{K}\cdot\hat{\mathbf{n}}|_y d\psi_2\approx\int_{-\infty}^{\infty}\frac{N_0(\Delta)}{(D_0+\Delta^2/D_m)^2}d\Delta=\frac{1}{2\pi}\ln\left(\frac{\sqrt{\epsilon}}{2\sigma_1}\right)+K_y^{(\mathrm{out})}(0). \tag{27}$$

As before, the outer contribution to the integral on scale ϕ_2/ϵ must be the same as that for the cusp expansion of Sec. III. This constant $K_y^{(\mathrm{out})}(0)$ has been calculated in Appendix B 2 for the special case of the Jeong-Moffatt geometry.

We can now verify that the interface shape (2), together with the tangential velocity (8), satisfies the integral equation (3) on the scale of the cusp. In the limit $\epsilon\to 0$ the external flow is once more

$$\mathbf{v}^{(\mathrm{ext})}=\left(O(\epsilon^{3/2}),\frac{9}{16\pi}\ln\frac{\sqrt{3}\epsilon}{16}+O(\epsilon)\right). \tag{28}$$

Thus, for the x component we have using Eqs. (22), (23), and (26) that

$$\frac{1}{4\pi}\ln\left(\frac{\epsilon}{4\sigma_1^2}\right)\frac{1+c\sigma_1^2}{\sigma_1}\sqrt{\epsilon}=\sqrt{\epsilon}\frac{1+c\sigma_1^2/3}{\pi\sigma_1}-\left[\frac{1+c\sigma_1^2/3}{\pi\sigma_1}+\frac{1+c\sigma_1^2}{2\pi\sigma_1}\ln\left(\frac{2\sigma_1}{\sqrt{\epsilon}}\right)\right]\sqrt{\epsilon},$$

which is satisfied for *any* c. This confirms that locally the cusp is determined up to a free constant c only, which then is set by the external flow and the boundary conditions.

As for the y-component, the corresponding balance is, using Eqs. (22), (24), and (27), that

$$\frac{1}{4\pi}\ln\left(\frac{\epsilon}{4\sigma_1^2}\right)=-\frac{1}{2\pi}\left[\ln\left(\frac{\epsilon\sigma_1^2}{2}\right)-1\right]-J_y^{(\mathrm{out})}(0)-\frac{1}{2\pi}\ln\left(\frac{\sqrt{\epsilon}}{2\sigma_1}\right)-K_y^{(\mathrm{out})}(0)+\frac{9}{16\pi}\ln\frac{\sqrt{3}\epsilon}{16}.$$

It is easy to check that the universal dependence on σ_1, which comes from the inner contribution to the integrals, is satisfied identically. The remaining constant is not universal, but it is easily confirmed that with the constants calculated in Appendix B 2, the equation is satisfied identically for the Jeong-Moffatt geometry.

V. CONCLUSIONS

In conclusion, we have shown that two-dimensional flows exhibiting free-surface cusps in the limit of strong driving, previously found using exact methods, have a universal structure that applies to any flow geometry. First, we have shown that the tip of the cusp, where the interface has a parabolic profile, is in itself an exact local solution to Stokes' equation, resulting from a balance of

viscous stresses and surface tension. This inner solution consists of the leading order expression of Eq. (1) for the interface shape, $x = \epsilon^2\psi$ and $y = \epsilon^2\psi^2/2$, together with the tangential velocity (7). Such a flow was considered already in the exact solution of Hopper [43], and suggests that the same type of local solution applies to the merging of cylinders [34], allowing for uniform translation [30,44].

Second, the intermediate self-similar solution (2) is driven by the point forcing exerted from the cusp tip, and the tangential velocity is described by Eq. (8). Third, the curvature of the tip of the cusp grows exponentially with the strength of the driving. If this strength of driving is described by the external velocity at the position of the cusp, as in Eq. (16), the both the exponent, as well as the prefactor, are nonuniversal, and depend on the details of the outer flow.

This is illustrated by another exact solution of the flow equations, describing an extensional flow around a two-dimensional "bubble" [11]. The external flow (C1), apart from the flow strength λ, contains a nonlinearity of amplitude c. As a result, the character of the flow can be varied, and the effect on cusp formation be studied. The calculation of the cusp curvature is described in detail in Appendix C. It is shown that in the asymptotic limit of large curvature, the tip curvature once more grows exponentially, cf. Eq. (C8). However, both the prefactor and the exponent depend on the parameter c, and hence cannot be universal. However, as demonstrated in Eq. (19), the exponent becomes universal if the capillary number is defined suitably as a flow speed in the *presence* of the cusp interface.

The advantage of having a local solution, as derived in the present paper, is that it may serve as a building block of a more complicated solution, for example containing several singularities, or existing in dimensions higher than two. As concerns the first possibility, out of two cusp singularities, a singularity of higher order can be constructed [22], which we expect can be shown to be a solution of free-surface Stokes flow using the same method as used here. As for higher dimensions, in practice no flow will be exactly two-dimensional. Instead, the flow intensity may vary in the third direction along the cusp line, as a result of which the two-dimensional solution "unfolds" [1] into the third dimension. Another interesting question concerns the transition between two-dimensional cusps (treated here), and three-dimensional, near conical tips [38], which one should be able to address with an understanding of the local cusp solution.

APPENDIX A: THE JEONG-MOFFATT SOLUTION

1. The free surface

In the exact solution of Ref. [2], the free surface is given by the complex mapping

$$w(\zeta) = a(\zeta + i) + (a+1)i\frac{\zeta - i}{\zeta + i}, \tag{A1}$$

where $\zeta = e^{i\theta}$. Taking the real and imaginary parts yields

$$x = a\cos\theta + \frac{(a+1)\cos\theta}{1+\sin\theta}, \quad y = a(\sin\theta - 1), \tag{A2}$$

where the y coordinate has been shifted so that $(x, y) = (0, 0)$ at the cusp $\theta = \pi/2$. Putting $a = -1/3 + \bar{\epsilon}$, where $\bar{\epsilon}$ is called ϵ in the notation of Ref. [2], the singularity is reached for $\bar{\epsilon} \to 0$. The mapping (A2) first becomes noninvertible for $\theta = \pi/2$, so to describe the neighborhood of the cusp, we put $\theta = \pi/2 - \varphi$ and expand in φ. Then the curvature, in units of the distance d between the double dipole and the free surface, is $\kappa = 4/(27\bar{\epsilon}^2)$; thus, $\bar{\epsilon} = (2/\sqrt{27})\epsilon$.

Expanding in $\bar{\epsilon}$ and φ, where we take $\varphi = O(\sqrt{\bar{\epsilon}})$, we have

$$x = \frac{3\bar{\epsilon}}{2}\varphi + \frac{\varphi^3}{12}, \quad y = \frac{\varphi^2}{6}.$$

To bring that into the form (1), we substitute $\varphi = \sqrt{3}\epsilon\psi$, from which we find $c = 3^{3/2}/4$.

2. The tangential velocity

We use the exact solution to find the velocity field in the limit of vanishing ϵ, which we then demonstrate to be part of a local solution to the integral equation (3). Since the interface is stationary, we only need the tangential velocity u_0. According to Ref. [2], Eq. (3.11), if α is the dipole strength driving the flow, this is

$$u_0 = -\frac{\alpha}{H(a)}(1+\sin\theta)\cos\theta|w'(e^{i\theta})|I(\sin\theta;a), \tag{A3}$$

where ($a<0$)

$$H = -\frac{a(3a+2)^2}{1+a+\sqrt{-2a(a+1)}}K(m)$$

and

$$I(\zeta;a) = \frac{4}{(t_1-\zeta)\left[a+1+\sqrt{-2a(a+1)}\right]}\left(K(m)-\frac{t1+1}{\zeta+1}\Pi(n,m)\right),$$

with

$$t_1 = \frac{-a(2a+1)+(a+1)\sqrt{-2a(a+1)}}{a(3a+2)}, \quad n = \frac{2(\zeta-t1)}{(\zeta+1)(1-t_1)},$$
$$m = \frac{2}{\left(-\frac{2a}{a+1}\right)^{1/4}+\left(-\frac{a+1}{2a}\right)^{1/4}},$$

where $K(m)$ and $\Pi(n,m)$ are the usual elliptic integrals of the first and third kinds, respectively, as defined in Ref. [45]. According to Ref. [2], Eq. (2.38), $\alpha/v_\eta = H(a)/4\pi$, where $v_\eta = \gamma/\eta$ is the capillary velocity, and so in units of v_η:

$$u_0 = -\frac{1}{4\pi}(1+\sin\theta)\cos\theta|w'(e^{i\theta})|I(\sin\theta;a). \tag{A4}$$

For ζ real between -1 and 1, $\Pi(n,m)$ has to be interpreted as a principal value. To avoid this, we first express $\Pi(n,m)$ through

$$R_J(x,y,z,p) = \frac{3}{2}\int_0^\infty \frac{dt}{(t+p)\sqrt{(t+x)(t+y)(t+z)}},$$

as defined in Ref. [46], and then use identity (6.11.21) of Ref. [46] to arrive at

$$\Pi(n,m) = K(m)+\frac{n}{3}R_j(0,1-m^2,1,1-n) = \frac{m^2}{m^2-n}K(m)+\frac{nm^2(1-m^2)}{3(m^2-n)^2}R_j(0,q,1,p),$$

where $q=1-m^2$ and $p=n(1-m^2)/(n-m^2)>1$. To obtain an approximation to $\Pi(n,m)$ that is uniform in θ, we rescale and then split the integral into two pieces:

$$R_j(0,q,1,p) = \frac{3}{2}\int_0^\infty \frac{dt}{(t+p)\sqrt{t(t+q)(t+1)}} = \frac{3}{2q^{3/2}}\int_0^\infty \frac{ds}{(s+r)\sqrt{s(s+1)(s+q^{-1})}}$$
$$= \frac{3}{2q^{3/2}}\left(\int_0^{q^{-1/2}} ds + \int_{q^{-1/2}}^\infty ds\right),$$

where $r=p/q=n/(n-m^2)$. Since $q=(3/16)\epsilon^2+O(\epsilon^3)$, for $\epsilon\to 0$ we can make the uniform approximations $s+q^{-1}\approx q^{-1}$ in the first integral, and $s+1\approx s$ in the second, which results in integrals which can be performed analytically to give

$$R_j(0,q,1,p) \approx \frac{3}{2q}I_1(q^{-1/2})+\frac{3}{2}I_2(q^{1/2}), \tag{A5}$$

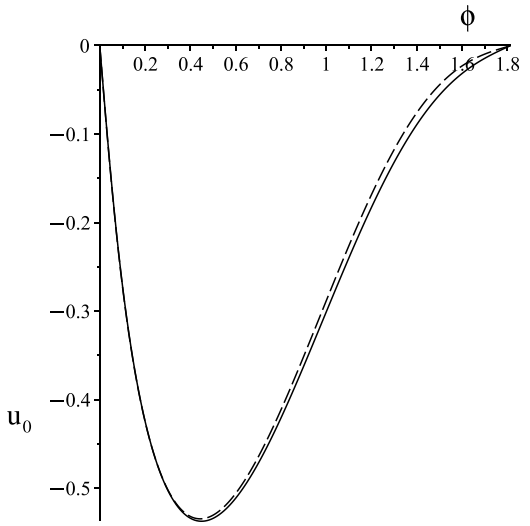

FIG. 3. The exact solution for the tangential velocity (A4), for $\epsilon = 0.1$ (solid line). The dashed line is the uniform approximation (A7).

where

$$I_1(s) = \frac{\operatorname{arccoth}\frac{2rs+r-s}{2\sqrt{r}\sqrt{r-1}\sqrt{s}\sqrt{s+1}}}{\sqrt{r}\sqrt{r-1}}, \quad I_2(t) = \frac{2\operatorname{arccoth}\frac{\sqrt{t+1}}{\sqrt{p-1}} + \ln\frac{\sqrt{t+1}-1}{\sqrt{t+1}+1}\sqrt{p-1}}{p\sqrt{p-1}}.$$

With these simplifications, we can now compute a series expansion of u_0 in ϵ at constant ψ; this yields Eq. (7) at leading order.

3. Matched asymptotic description

It is instructive to represent the tangential velocity, using the expansions implied by Eqs. (10) and (11), to obtain a uniformly valid expression. The inner expansion is given by Eq. (7), the outer expansion follows from taking the limit of Eq. (A4) as $\epsilon \to 0$ at constant ϕ, using the approximation (A5). The result is

$$u_0^{(\mathrm{out})}(\phi) = \frac{\mathrm{s}\sqrt{5-3\mathrm{c}^2-2\mathrm{c}}}{4\pi(1-\mathrm{c})}\ln\epsilon + \frac{\mathrm{s}}{\pi\sqrt{1-\mathrm{c}^2}(1-\mathrm{c})} \times\left[\frac{1-\mathrm{c}}{2}\operatorname{arccoth}\left(\frac{9-7\mathrm{c}^2-2\mathrm{c}}{4\mathrm{s}\sqrt{5+3\mathrm{c}}\sqrt{1-\mathrm{c}}}\right) - \sqrt{5-3\mathrm{c}^2-2\mathrm{c}}\sqrt{1-\mathrm{c}^2}\left(\ln 2 - \frac{\ln 3}{8}\right)\right], \tag{A6}$$

having put $\mathrm{c} = \cos(\sqrt{3}\phi)$ and $\mathrm{s} = \sin(\sqrt{3}\phi)$ for brevity. Expanding the inner expansion (7) for large ϕ, and the outer expansion (A6) for small ϕ, one obtains the description (8), valid in the overlap region. In other words,

$$u_0(\phi) \approx -\frac{1}{\pi}\ln\left(\sqrt{1+(\phi/\epsilon)^2}+\phi/\epsilon\right) + u_0^{(out)}(\phi) + \frac{1}{\pi}\ln\frac{2\phi}{\epsilon} \tag{A7}$$

is a uniform approximation, valid in the limit $\epsilon \to 0$. As seen in Fig. 3, it already works quite well for $\epsilon = 0.1$; for $\epsilon = 0.01$ the two curves are virtually indistinguishable. In the limit of small ϕ,

expanding $u_0^{(\mathrm{out})}(\phi)$, Eq. (A7) becomes

$$u_0(\phi) \approx -\frac{1}{\pi}\ln\left(\sqrt{1+(\phi/\epsilon)^2}+\phi/\epsilon\right) - \frac{21}{32\pi}\phi^2\ln\epsilon + \frac{168\ln 2 - 21\ln 3 - 13}{64\pi}\phi^2 + O(\phi^4). \tag{A8}$$

APPENDIX B: CALCULATION OF INTEGRALS

1. Inner integrals

In the following, we focus on the x component, but the y component can be treated in a similar fashion. In the inner expansion, for the integrand of the J integral we find to leading order in ϵ that

$$\begin{aligned}\kappa\mathbf{J}\cdot\hat{\mathbf{n}}|_x =& -\frac{\psi_2}{8\pi\left(1+\psi_2^2\right)^{3/2}}\ln\left[\left((\psi_1+\psi_2)^2+4\right)(\psi_1-\psi_2)^2\right] \\ &+\frac{1}{2\pi}\frac{\psi_2-\psi_1}{\left(1+\psi_2^2\right)^{3/2}[(\psi_1+\psi_2)^2+4]} + \frac{\psi_2\ln(2/\epsilon^2)}{4\pi\left(1+\psi_2^2\right)^{3/2}}\end{aligned} \tag{B1}$$

and

$$\begin{aligned}\kappa\mathbf{J}\cdot\hat{\mathbf{n}}|_y =& \frac{\ln(\epsilon^2/2)}{4\pi\left(1+\psi_2^2\right)^{3/2}} + \frac{\ln\left[\left((\psi_1+\psi_2)^2+4\right)(\psi_1-\psi_2)^2\right]}{8\pi\left(1+\psi_2^2\right)^{3/2}} \\ &+\frac{\psi_2^2-\psi_1^2}{4\pi\left(1+\psi_2^2\right)^{3/2}[(\psi_1+\psi_2)^2+4]}.\end{aligned} \tag{B2}$$

The K-integral, however, yields for the inner expansion:

$$\mathbf{v}\cdot\mathbf{K}\cdot\hat{\mathbf{n}}|_x = \frac{4u_0(\psi_2)}{\pi}\frac{\psi_2(\psi_1+\psi_2)+2}{\left(1+\psi_2^2\right)^{1/2}[(\psi_1+\psi_2)^2+4]^2} \tag{B3}$$

and

$$\mathbf{v}\cdot\mathbf{K}\cdot\hat{\mathbf{n}}|_y = \frac{2u_0(\psi_2)}{\pi}\frac{(\psi_1+\psi_2)(\psi_2(\psi_1+\psi_2)+2)}{\left(1+\psi_2^2\right)^{1/2}[(\psi_1+\psi_2)^2+4]^2}. \tag{B4}$$

We focus on verifying Eq. (13); Eq. (14) is treated similarly. To this end we split Eq. (13) up in the form

$$-\frac{\operatorname{arcsinh}(\psi_1)}{\sqrt{1+\psi_1^2}} = -J_{x1}+J_{x21}+J_{x22}+K_x, \tag{B5}$$

where

$$\begin{aligned}J_{x1} &= \int_{-\infty}^{\infty}\frac{\psi_2-\psi_1}{(1+\psi_2^2)^{3/2}[(\psi_1+\psi_2)^2+4]}d\psi_2, \\ J_{x21} &= \int_{-\infty}^{\infty}\frac{\psi_2\ln((\psi_1+\psi_2)^2+4)}{4\left(1+\psi_2^2\right)^{3/2}}d\psi_2, \\ J_{x22} &= \int_{-\infty}^{\infty}\frac{\psi_2\ln|\psi_1-\psi_2|}{2\left(1+\psi_2^2\right)^{3/2}}d\psi_2, \\ K_x &= \int_{-\infty}^{\infty}\frac{8\operatorname{arcsinh}(\psi_2)}{\pi\sqrt{1+\psi_2^2}}\frac{\psi_2(\psi_1+\psi_2)+2}{[(\psi_1+\psi_2)^2+4]^2}d\psi_2.\end{aligned}$$

The contribution J_{x1} is of the form

$$\int \frac{P(x)}{Q(x)\sqrt{1+x^2}^n}dx, \tag{B6}$$

where $P(x)$ and $Q(x)$ are polynomials, so that primitives can be found using a method described in Ref. [45]. We calculated the definite integral J_{x1} in terms of elementary functions, using MAPLE. The contributions from J_{x21} and J_{x22} are simplified integrating by parts, the result is

$$J_{x21} = \int_{-\infty}^{\infty} \frac{(\psi_1+\psi_2)}{2[(\psi_1+\psi_2)^2+4]\sqrt{1+\psi_2^2}}d\psi_2,$$

which MAPLE integrates in terms of elementary functions. To calculate J_{x22}, we note

$$\begin{aligned}\int \frac{\psi_2 \ln|\psi_1-\psi_2|}{\left(1+\psi_2^2\right)^{3/2}}d\psi_2 &= \int \frac{d\psi_2}{(\psi_2-\psi_1)\sqrt{1+\psi_2^2}} - \frac{\ln|\psi_1-\psi_2|}{\sqrt{1+\psi_2^2}} \\ &= -\frac{\operatorname{arcsinh}\frac{1+\psi_1\psi_2}{|\psi_1-\psi_2|}}{\sqrt{1+\psi_1}} - \frac{\ln|\psi_1-\psi_2|}{\sqrt{1+\psi_2^2}},\end{aligned}$$

from which we find

$$J_{x22} = -\frac{\operatorname{arcsinh}\psi_1}{\sqrt{1+\psi_1^2}},$$

which cancels the left-hand side of Eq. (B5).

Finally, K_x, whose integrand has branch points at $z=\pm i$, can be simplified using contour integration. We choose branch cuts that extend from $\pm i$ to infinity along the imaginary axis, so that for $z=it$,

$$\sqrt{1+z^2} = \pm i\sqrt{t^2-1}, \quad \operatorname{arcsinh}(z) = \frac{i\pi}{2} \pm \ln\left(\sqrt{t^2-1}+t\right),$$

to the right and left of the upper branch cut, respectively. Further, the integrand has a pole at $\psi_2 = 2i-\psi_1$. Thus, choosing as the contour the real axis, plus a circle at infinity, avoiding the upper branch cut, one finds

$$K_x = -8\Im\left\{\int_1^{\infty} \frac{2+it(\psi_1+it)dt}{\sqrt{t^2-1}[(\psi_1+it)^2+4]^2}\right\} - 2\pi\Im\{\operatorname{Res}(f,\psi_2=2i-\psi_1)\},$$

where $f(\psi_2)$ is the integrand of K_x.

The integral over t can again be performed in terms of elementary functions, using MAPLE, which shows that indeed

$$K_x = J_{x1} - J_{x21},$$

which demonstrates Eq. (B5) and thus Eq. (13).

2. Constants in the integral equation

In the y component of the integral equation (14), we have computed integrals up to constants only, since the constants depend on the particular problem at hand. However, as a test of our method, it is instructive to calculate all constants based on the exact solution [2], and to verify Eq. (15).

Beginning with the left-hand side of Eq. (15), the external flow is

$$u - iv = -\frac{i\alpha}{(z+i)^2} = -v_\eta \frac{iH(a)}{4\pi(z+i)^2}, \quad H(a) \approx \ln(32/(9\bar{\epsilon}))/4 = \ln(16/(\sqrt{3}\epsilon))/4, \tag{B7}$$

and the tip of the cusp is at $z = 2ai = (-2/3 + 2\bar{\epsilon})i$. Thus, to leading order, in units of v_η, the y component of the external velocity is

$$v^{(\mathrm{ext})} = \frac{9}{16\pi}\left(\ln\epsilon + \ln\frac{\sqrt{3}}{16}\right). \tag{B8}$$

The integrals on the right-hand side of Eq. (15) go from $\varphi = -\pi$ to $\varphi = \pi$, so with $\theta = \pi/2 - \sqrt{3}\epsilon\psi$ and the inner/outer expansion $f(\psi_2) = f_0(\psi_2) + F_1(\phi_2)\epsilon$ we have

$$\begin{aligned}\int_{-\pi/(\sqrt{3}\epsilon)}^{\pi/(\sqrt{3}\epsilon)} f(\psi_2)d\psi_2 &= \int_{-\pi/(\sqrt{3}\epsilon)}^{\pi/(\sqrt{3}\epsilon)} f_0(\psi_2)d\psi_2 + \int_{-\pi/(\sqrt{3}\epsilon)}^{\pi/(\sqrt{3}\epsilon)} F_1(\phi_2)d\psi_2 \\ &= \int_{-\infty}^{\infty} f_0(\psi_2)d\psi_2 + \int_{-\pi/\sqrt{3}}^{\pi/\sqrt{3}} F_1(\phi_2)d\phi_2,\end{aligned}$$

having taken the limit $\epsilon \to 0$ and substituting $\psi_2 = \phi_2/\epsilon$ in the second step. The inner expansion f_0 for both J and K integrals is universal, and determined by the cusp tip alone. Thus, the inner integrand for the J integral is

$$f_0^{(Jy)} = \frac{\ln(\psi_2^2(\psi_2^2+4))\psi_2^2 - 2\ln(2)\psi_2^2 + 2\psi_2^2 + 4\ln(\psi_2^2(\psi_2^2+4)) - 8\ln(2)}{8(\psi_2^2+1)^{3/2}(\psi_2^2+4)\pi} + \frac{\ln\epsilon}{2\pi(\psi_2^2+1)^{3/2}},$$

see Eq. (23). However, for the K integral:

$$f_0^{(Ky)} = -\frac{2\ln\left(\sqrt{2+\psi_2^2}+\psi_2\right)\psi_2(\psi_2^2+2)}{\pi^2\sqrt{1+\psi_2^2}(4+\psi_2^2+4)^2}.$$

Next, in the outer expansion, to compute F_1, the full expressions for the shape, and Eq. (A4) for the tangential velocity, using the approximation (A5), are evaluated in the limit $\epsilon \to 0$ at constant ϕ. The results are

$$\begin{aligned}F_1^{(Jy)} = &\frac{6\sqrt{3}\mathrm{s}(1+\mathrm{c})}{\pi\sqrt{5+3\mathrm{c}^2+8\mathrm{c}}(24\mathrm{c}+40)} \\ &\times\left[\frac{2+\mathrm{c}}{2}\ln\frac{(1+\mathrm{c})^2}{(1-\mathrm{c})\mathrm{s}^2} + (1/2 - \ln(2)/2 + \ln(3))\mathrm{c} - \ln(2) + 2\ln(3) + 1/2\right],\end{aligned}$$

and

$$F_1^{(Ky)} = -\frac{3(3+\mathrm{c})\mathrm{s}}{4\pi\sqrt{15-9\mathrm{c}^2-6\mathrm{c}}}u_0^{(\mathrm{out})}(\phi),$$

for the J and K integrals, respectively; here $u_0^{(\mathrm{out})}$ is the tangential velocity given by Eq. (A6). We have once more abbreviated $\mathrm{c} = \cos(\sqrt{3}\phi)$ and $\mathrm{s} = \sin(\sqrt{3}\phi)$. For a numerical evaluation, it is useful to note that the K integrand has an expansion for small ϕ that reads

$$F_1^{(Ky)} = \frac{(\ln 2 + \ln\phi)\sqrt{3}}{2\pi^2} - \frac{\sqrt{3}(198\ln 2 + 30\ln\phi - 13 - 21\ln 3)\phi^2}{128\pi^2} + O(\phi^4).$$

Coming to the integrals, the contributions proportional to $\ln\epsilon$ are

$$2\int_0^\infty \frac{\ln\epsilon}{2\pi\left(1+\psi_2^2\right)^{3/2}} = \frac{\ln\epsilon}{\pi} \tag{B9}$$

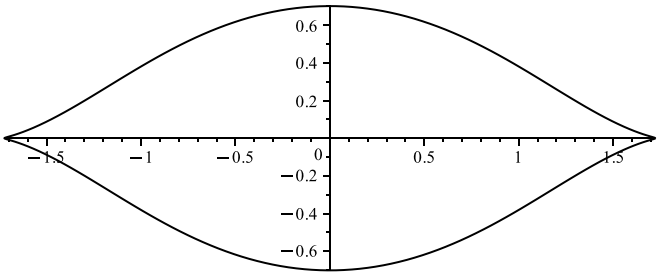

FIG. 4. A two-dimensional "bubble" in the flow (C1), as described by Eq. (C2). Parameters are $\beta = 0.22$ and $c = 1$, from which follows $\alpha = 1.090155464$, $\lambda = 0.3252008219$, and $\kappa = 1171.7\ldots$.

for the inner J integral, and

$$-\frac{3\ln\epsilon}{8\pi^2}\int_0^{\pi/\sqrt{3}}(c^2+4c+3)d\phi\ln\epsilon = -\frac{7}{16\pi}\ln\epsilon \tag{B10}$$

for the outer K integral. Since the numerical values of the remaining constants are not very significant for our purposes, we have not attempted to calculate them analytically. Numerically, we find for the inner integrals that

$$J_y^{(\mathrm{in})}(0) = -0.06130418454 + \ln\epsilon/\pi, \quad K_y^{(\mathrm{in})}(0) = -0.4288041588;$$

these are universal numbers, in view of the universal nature of the inner expansion. For the outer integrals, a numerical evaluation of integrals yields

$$J_y^{(\mathrm{out})}(0) = 0.2112196778, \quad K_y^{(\mathrm{out})}(0) = -0.119188 - 7\ln\epsilon/(16\pi).$$

It is easy to check that this satisfies Eq. (15) to the precision at which the integrals were computed, as required.

APPENDIX C: THE ANTANOVSKII SOLUTION

Following Ref. [11], we consider a two-dimensional "bubble" of undeformed (circular) radius R in the nonlinear extensional flow

$$u^{(\mathrm{ext})} = \frac{\lambda}{2}\big[x + cx(x^2+3y^2)\big], \quad v^{(\mathrm{ext})} = -\frac{\lambda}{2}\big[y - cy(3x^2+y^2)\big]; \tag{C1}$$

We take units of length to be R, and $R\eta/\gamma$ to be units of time. The bubble is described by the complex mapping

$$z = \frac{\alpha+\beta\zeta^2}{\zeta(1-\gamma\zeta^2)}, \quad \zeta = e^{i\theta}, \tag{C2}$$

where α, β, γ are real parameters. It has been shown [11] that

$$\alpha = \sqrt{\frac{2(1+\beta^2)}{A_c(\beta)+\big[A_c^2(\beta)-B_c^2(\beta)\big]^{1/2}}}, \quad \gamma = c\alpha\beta, \tag{C3}$$

where $A_c(\beta) = 1 - c\beta^2[2(1-c)+c\beta^2]$ and $B_c(\beta) = 4c^2\beta^2(1+\beta^2)[3+c(2+c)\beta^2]$. Then the strength of the flow is given by

$$\lambda = \frac{\beta}{\pi\alpha}\int_0^{\pi}\frac{d\theta}{|\alpha(1-3\gamma e^{i\theta})-\beta e^{i\theta}(1+\gamma e^{i\theta})|}. \tag{C4}$$

An example of a bubble shape is shown in Fig. 4, which develops near cusps at either ends. Expanding about $\theta = 0$, one finds to leading order the generic cusp

$$x = a_0 + a_2\theta^2, \quad y = b_1\theta + b_3\theta^3, \tag{C5}$$

with $a_0 = (\alpha + \beta)/(1 - \gamma)$ the position of the cusp tip, and

$$a_2 = \frac{(9\alpha + \beta)\gamma^2 + (6\beta - 2\alpha)\gamma + \alpha + \beta}{2(\gamma - 1)^3}, \quad b_1 = \frac{(\beta + 3\alpha)\gamma + \beta - \alpha}{(\gamma - 1)^2},$$
$$b_3 = \frac{(-\beta - 27\alpha)\gamma^3 + (-23\beta - 17\alpha)\gamma^2 + (-23\beta - 5\alpha)\gamma - \beta + \alpha}{6(\gamma - 1)^4}.$$

Thus, the formation of the cusp is once more associated with the interface self-intersecting. The curvature κ diverges for $b_1 \to 0$, and its value is

$$\kappa = -\frac{2a_2}{b_1^2} = \frac{[(9\alpha + \beta)\gamma^2 + (-2\alpha + 6\beta)\gamma + \alpha + \beta](1 - \gamma)}{\Delta^2}, \tag{C6}$$

with $\Delta = \alpha - \beta - \gamma(3\alpha + \beta)$.

1. The curvature

We want to calculate the curvature as a function of flow strength. To this end we evaluate the integral (C4) in the limit $\Delta \to 0$. Writing the integrand in the form $f(\theta, \Delta)$ and expanding in Δ, one finds $f = F_0(\theta) + O(\Delta)$, with

$$F_0 = \frac{3\alpha + \beta}{\sqrt{8\cos(\theta)^2\alpha^2\beta^2 - 2(3\alpha^2 + \beta^2)^2\cos(\theta) + (12\alpha^3\beta - 4\alpha\beta^3)\sin(\theta)^2 + 2\beta^4 + 4\alpha^2\beta^2 + 18\alpha^4}}.$$

But F_0 diverges like $1/\theta$ for small θ, so we need an inner expansion in Δ, but at constant $\xi = \theta/\Delta$: $f = f_{-1}(\xi)\Delta + \ldots$. The inner limit of the outer expansion

$$O_1 = \frac{1}{\Delta}\frac{3\alpha + \beta}{(\alpha + \beta)(3\alpha + \beta)}$$

coincides with the outer limit of the inner expansion, which is

$$f_{-1} = \frac{3\alpha + \beta}{\sqrt{(3\alpha + \beta)^2 + (\alpha^2 + \beta^2)^2(3\alpha - \beta)\xi^2}}.$$

Thus, we can write

$$\lambda = \frac{\beta}{\pi\alpha}\left[\int_0^\pi (F_0 - O_1)d\theta + \int_0^\pi f_{-1}d\xi\right],$$

which results in

$$\lambda = \ell_0 \ln\left[\frac{4(\alpha + \beta)(3\alpha - \beta)(\pi + \sqrt{\pi^2 + a})}{\pi(3\alpha^2 + \beta^2)a}\right] \approx \ell_0 \ln(d_1/\Delta), \tag{C7}$$

where $a = (3\alpha + \beta)\Delta/[(\alpha + \beta)(3\alpha - \beta)]$, and

$$\ell_0 = \frac{\beta(3\alpha + \beta)}{\pi\alpha(\alpha + \beta)(3\alpha - \beta)}, \quad d_1 = \frac{8(\alpha + \beta)^2(3\alpha - \beta)^2}{[(3\alpha^2 + \beta^2)(3\alpha + \beta)]},$$

expanding in Δ. Hence, finally, in the limit of large curvatures,

$$\kappa = \frac{\left(3\alpha^2 + \beta^2\right)^2}{2(3\alpha - \beta)^3(\alpha + \beta)(3\alpha + \beta)} \exp\left\{\frac{32\pi\alpha^2}{(3\alpha + \beta)^2}\mathrm{Ca}\right\}, \tag{C8}$$

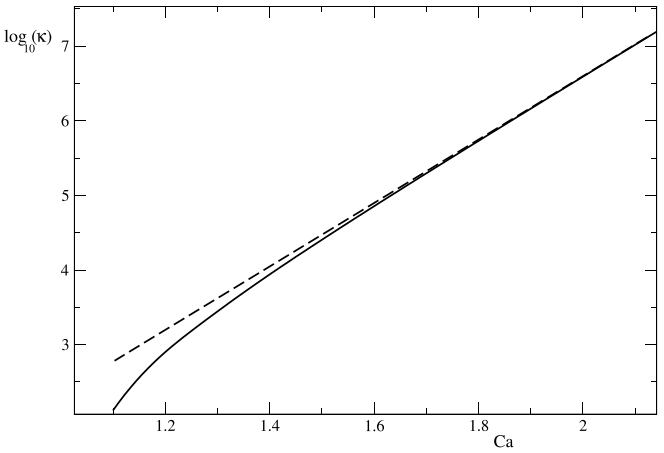

FIG. 5. The logarithm of the curvature as a function of Ca for Antanovskii's solution, holding $c = 1$ fixed. The solid line is a numerical solution of Antanovskii's solution using Eqs. (C6) and (C4); the dashed line is the approximation (C8), with $\alpha = 1.101072\ldots$ and $\beta = 0.2253872\ldots$, leading to $\kappa \approx 0.011245756e^{9.789\mathrm{Ca}}$.

where Ca is the external velocity (C1), in units of γ/η, evaluated at the position of the cusp. Here α, β are to be evaluated for fixed c, with $\Delta = 0$. Figure 5 demonstrates that this captures the exponential asymptotics of the curvature exactly. Clearly, the coefficients appearing in Eq. (C8) are not universal but depend on c (and they differ from those of Jeong and Moffatt's solution [2]). For example, for $c = 0.1$ the result is $\kappa \approx 0.01265e^{7.79547\mathrm{Ca}}$, while for $c = 1$, $\kappa \approx 0.01246e^{9.7887\mathrm{Ca}}$.

[1] J. Eggers and M. A. Fontelos, *Singularities: Formation, Structure, and Propagation* (Cambridge University Press, Cambridge, UK, 2015).

[2] J.-T. Jeong and H. K. Moffatt, Free-surface cusps associated with a flow at low Reynolds numbers, J. Fluid Mech. **241**, 1 (1992).

[3] D. D. Joseph, J. Nelson, M. Renardy, and Y. Renardy, Two-dimensional cusped interfaces, J. Fluid Mech. **223**, 383 (1991).

[4] É. Lorenceau, F. Restagno, and D. Quéré, Fracture of a viscous liquid, Phys. Rev. Lett. **90**, 184501 (2003).

[5] J. Eggers, Air entrainment through free-surface cusps, Phys. Rev. Lett. **86**, 4290 (2001).

[6] E. Lorenceau, D. Quéré, and J. Eggers, Air entrainment by a viscous jet plunging into a bath, Phys. Rev. Lett. **93**, 254501 (2004).

[7] E. Reyssat, E. Lorenceau, F. Restagno, and D. Quéré, Viscous jet drawing air into a bath, Phys. Fluids **20**, 091107 (2008).

[8] J.-T. Jeong, Two-dimensional Stokes flow due to a pair of vortices below the free surface, Phys. Fluids **22**, 082102 (2010).

[9] J.-T. Jeong, Formation of cusp on the free surface at low Reynolds number flow, Phys. Fluids **11**, 521 (1999).

[10] J.-T. Jeong, Free-surface deformation due to a source or sink in Stokes flow, Eur. J. Mech. B Fluids **26**, 720 (2007).

[11] L. K. Antanovskii, Formation of a pointed drop in Taylor's four-roller mill, J. Fluid Mech. **327**, 325 (1996).

[12] D. Crowdy, Exact solutions for two steady inviscid bubbles in the slow viscous flow generated by a four-roller mill, J. Engin. Math. **44**, 311 (2002).

[13] L. J. Cummings, Steady solutions for bubbles in dipole-driven stokes flows, Phys. Fluids **12**, 2162 (2000).

[14] L. J. Cummings and S. D. Howison, Two-dimensional Stokes flow with suction and small surface tension, Eur. J. Appl. Math. **10**, 681 (1999).
[15] K. T. Kiger and J. H. Duncan, Air-entrainment mechanisms in plunging jets and breaking waves, Annu. Rev. Fluid Mech. **44**, 563 (2012).
[16] A. E. Hosoi and L. Mahadevan, Axial instability of a free-surface front in a partially filled horizontal rotating cylinder, Phys. Fluids **11**, 97 (1999).
[17] G. I. Taylor, The formation of emulsions in definable fields of flow, Proc. R. Soc. London A **146**, 501 (1934).
[18] S. C. du Pont and J. Eggers, Sink flow deforms the interface between a viscous liquid and air into a tip singularity, Phys. Rev. Lett. **96**, 034501 (2006).
[19] S. C. du Pont and J. Eggers, Fluid interfaces with very sharp tips in viscous flow, Proc. Natl. Acad. Sci. USA **117**, 32238 (2020).
[20] O. Hassager, Negative wake behind bubbles in non-Newtonian liquids, Nature (London) **279**, 402 (1979).
[21] J. Eggers and M. A. Fontelos, Cusps in interfacial problems, Panoramas et Synthèses **38**, 69 (2012).
[22] J. Eggers and N. Suramlishvili, Singularity theory of plane curves and its applications, Eur. J. Mech. B Fluids **65**, 107 (2017).
[23] L. D. Landau and E. M. Lifshitz, *Elasticity* (Pergamon, Oxford, UK, 1984).
[24] S. Karpitschka, J. Eggers, A. Pandey, and J. H. Snoeijer, Cusp-shaped elastic creases and furrows, Phys. Rev. Lett. **119**, 198001 (2017).
[25] A. Chakrabarti, T. C. T. Michaels, S. Yin, E. Sun, and L. Mahadevan, The cusp of an apple, Nat. Phys. **17**, 1125 (2021).
[26] J. Nye, *Natural Focusing and Fine Structure of Light: Caustics and Wave Dislocations* (Institute of Physics Publishing, Bristol, UK, 1999).
[27] J. Eggers, J. Hoppe, M. Hynek, and N. Suramlishvili, Singularities of relativistic membranes, Geometric Flows **1**, 17 (2015).
[28] J. Eggers, T. Grava, M. A. Herrada, and G. Pitton, Spatial structure of shock formation, J. Fluid Mech. **820**, 208 (2017).
[29] C. Kamal, J. Sprittles, J. H. Snoeijer, and J. Eggers, Dynamic drying transition via free-surface cusps, J. Fluid Mech. **858**, 760 (2019).
[30] S. D. Howison, J. D. Morgan, and J. R. Ockendon, A class of codimension-two free boundary problems, SIAM Rev. **39**, 221 (1997).
[31] J. D. Morgan, Codimension-two free boundary problems, Ph.D. thesis, Oxford University, 1994.
[32] K. Gillow, Codimension-two free boundary problems, Ph.D. thesis, Oxford University, 1998.
[33] G. K. Batchelor, *An Introduction to Fluid Dynamics* (Cambridge University Press, Cambridge, UK, 1967).
[34] R. W. Hopper, Plane Stokes flow driven by capillarity on a free surface, J. Fluid Mech. **213**, 349 (1990).
[35] S. Richardson, Two-dimensional slow viscous flows with time-dependent free boundaries driven by surface tension, Eur. J. Appl. Math **3**, 193 (1992).
[36] J. M. Rallison and A. Acrivos, A numerical study of the deformation and burst of a viscous drop in an extensional flow, J. Fluid Mech. **89**, 191 (1978).
[37] J. Tanzosh, M. Manga, and H. A. Stone, Boundary integral methods for viscous free-boundary problems: Deformation of single and multiple fluid-fluid interfaces, in *Proceedings of Boundary Element Technologies VII*, edited by C. A. Brebbia and M. S. Ingber (Computational Mechanics, Southhampton, 1992), p. 19.
[38] J. Eggers, Theory of bubble tips in strong viscous flows, Phys. Rev. Fluids **6**, 044005 (2021).
[39] C. Pozrikidis, *Boundary Integral and Singularity Methods for Linearized Flow* (Cambridge University Press, Cambridge, UK, 1992).
[40] E. J. Hinch, *Perturbation Methods* (Cambridge University Press, Cambridge, UK, 1991).
[41] J. P. K. Tillett, Axial and transverse Stokes flow past slender axisymmetric bodies, J. Fluid Mech. **44**, 401 (1970).
[42] M. Van Dyke, *Perturbation Methods in Fluid Mechanics* (The Parabolic Press, Stanford, CA, 1975).
[43] R. W. Hopper, Capillarity-driven plane Stokes flow exterior to a parabola, Q. J. Mech. appl. Math. **46**, 193 (1993).

[44] S. D. Howison and S. Richardson, Cusp development in free boundaries, and two-dimensional slow viscous flows, Eur. J. Appl. Math **6**, 441 (1995).
[45] I. S. Gradshteyn and I. M. Ryzhik, *Table of Integrals Series and Products* (Academic Press, New York, NY, 1980).
[46] W. H. Press, S. A. Teukolski, W. T. Vetterling, and B. P. Flannery, *Numerical Recipes* (Cambridge University Press, Cambridge, UK, 1992).